

High Density Behaviour of Nuclear Symmetry Energy and High Energy Heavy-Ion Collisions

Bao-An Li*

Department of Chemistry and Physics

P.O. Box 419, Arkansas State University

State University, Arkansas 72467-0419, USA

High energy heavy-ion collisions are proposed as a novel means to obtain information about the high density (HD) behaviour of nuclear symmetry energy. Within an isospin-dependent hadronic transport model using phenomenological equations of state (EOS) for dense neutron-rich matter, it is shown that the isospin asymmetry of the HD nuclear matter formed in high energy heavy-ion collisions is determined mainly by the HD behaviour of nuclear symmetry energy. Experimental signatures in several sensitive probes, i.e., π^- to π^+ ratio, transverse collective flow and its excitation function as well as neutron-proton differential flow, are investigated. A precursor of the possible isospin separation instability in dense neutron-rich matter is predicted to appear as the local minima in the excitation functions of the transverse flow parameter for both neutrons and protons above the pion production threshold. Because of its *qualitative* nature unlike other *quantitative* observables, this precursor can be used as a unique signature of the isospin dependence of the nuclear EOS. Measurements of these observables will provide the first terrestrial data to constrain stringently the HD behaviour of nuclear symmetry energy and thus also the EOS of dense neutron-rich matter. Implications of our findings to neutron star studies are also

*email: Bali@astate.edu

discussed.

PACS numbers: 25.70.-z, 25.75.Ld., 24.10.Lx

Key Words:High Energy Heavy Ion Collisions, Isospin, Symmetry Energy, Equation of State, Neutron-Rich Matter, Neutron Stars, Collective Flow

I. INTRODUCTION

The rapid advance in nuclear reactions using rare isotopes has opened up several new frontiers in nuclear sciences [1–8]. In particular, the intermediate energy heavy rare isotopes currently available at the National Superconducting Cyclotron Laboratory (NSCL/MSU) and the more energetic ones to be available at the future Rare Isotope Accelerator (RIA) in the United States provide a unique opportunity to explore novel properties of dense neutron-rich matter that was not in reach in terrestrial laboratories before. This exploration will reveal crucial information about the equation of state (EOS) of neutron-rich matter. To understand the latter and its astrophysical implications, such as, the origin of elements, structure of rare isotopes and properties of neutron stars are presently among the most important goals of nuclear sciences. The EOS of neutron-rich matter of isospin asymmetry $\delta \equiv (\rho_n - \rho_p)/(\rho_n + \rho_p)$ can be written as

$$e(\rho, \delta) = e(\rho, 0) + E_{sym}(\rho)\delta^2 \quad (1)$$

within the parabolic approximation (see e.g., [9]), where $e(\rho, 0)$ is the energy per nucleon in isospin symmetric nuclear matter. To study the density dependence of nuclear symmetry energy $E_{sym}(\rho)$ has been a longstanding goal of extensive research with various microscopic and/or phenomenological models over the last few decades, e.g., [10–22], for a recent review, see, e.g. [9]. All models are able to give the symmetry energy at normal nuclear matter density $E_{sym}(\rho_0)$ of about 34 ± 4 MeV in agreement with that extracted from the atomic mass data. However, the predicted results on the density dependence, especially at high densities, are extremely diverse and often contradictory. At subnormal densities, all models predict that the symmetry energy increase with density although the growing rate is rather model dependent. To extract the density dependence of symmetry energy at low densities, several approaches have recently been proposed. These include measuring the thickness of neutron-skins of rare isotopes [23] and heavy stable nuclei, such as ^{208}Pb [24–27], isospin fractionation [28–30] as well as nuclear collective flow [31–33] in intermediate energy heavy-ion collisions.

Above normal nuclear matter densities, even the trend of the density dependence of $E_{sym}(\rho)$ is still controversial. Theoretical results can be roughly classified into two groups, i.e., a group where the $E_{sym}(\rho)$ rises monotonously and one in which it falls with the increasing density above about twice the normal nuclear matter density. The predictions also depend on the nature and form of effective interactions used. For instance, within the same Hartree-Fock approach using about 25 Skyrme and Gony effective interactions that have been widely used successfully in studying saturation properties of symmetric nuclear matter and nuclear structures near the β stability valley, the calculated symmetry energies were found to fall approximately equally into the two groups [24,34].

The density dependence of nuclear symmetry energy, especially at high densities [35], has many profound consequences for various studies in astrophysics [36–38]. In particular, an increasing $E_{sym}(\rho)$ leads to a relatively more proton-rich neutron star whereas a decreasing one would make the neutron star a pure neutron matter at high densities. Consequently, the chemical composition and cooling mechanisms of protoneutron stars [39,40], critical densities for Kaon condensations in dense stellar matter [41,42], mass-radius correlations [43,44] as well as the possibility of a mixed quark-hadron phase [45] in the cores of neutron stars will all be rather different. The high density (HD) behaviour of nuclear symmetry energy $E_{sym}(\rho)$ is very important for understanding many interesting astrophysical phenomena, but it also subjects to the worst uncertainty among all properties of dense nuclear matter [35]. The fundamental cause of the extremely uncertain HD behaviour of $E_{sym}(\rho)$ is the complete lack of terrestrial laboratory data to constrain directly the model predictions. We explore in this work the possibility of using high energy heavy-ion collisions to probe the HD behaviour of $E_{sym}(\rho)$. A brief report of this work can be found in ref. [46]. The $E_{sym}(\rho)$ is found to affect significantly several aspects of high energy heavy-ion collisions. In particular, the neutron/proton ratio of HD nuclear matter formed in these collisions is determined mainly by the HD behaviour of $E_{sym}(\rho)$. Several promising signatures of the HD behaviour of $E_{sym}(\rho)$ are also investigated. Besides the *quantitative* observables, we also study one special *qualitative* signature of the HD behaviour of the symmetry energy, i.e., the local minimum

in the excitation function of nuclear transverse flow. The paper is organized as follows. In Section 2, we discuss the equation of state (EOS) for neutron-rich matter, in particular, the HD behaviour of nuclear symmetry and its effects on the neutron/proton ratio in neutron stars. In section 3, we study the neutron/proton ratio and its dependence on the symmetry energy in HD hadronic matter formed in high energy heavy-ion collisions within an isospin-dependent hadronic transport model. In section 4, we explore several experimental probes of the HD behaviour of nuclear symmetry energy. Finally, we summarize in section 5.

II. EQUATION OF STATE OF DENSE NEUTRON-RICH MATTER

In this section properties of the equation of state of dense neutron-rich matter are discussed. In particular, we discuss the HD behaviour of nuclear symmetry energy and potentials as well as their influences on neutron stars. Based on these properties, we present our expectations about their influences on heavy-ion collisions involving neutron-rich nuclei.

A. High density behaviour of nuclear symmetry energy

In the parabolic approximation of the EOS for neutron-rich matter in Eq. 1, the symmetry energy is [17]

$$E_{sym}(\rho) \equiv e(\rho, 1) - e(\rho, 0) = \frac{5}{9}E_{kin}(\rho, 0) + V_2(\rho), \quad (2)$$

where $E_{kin}(\rho, 0)$ is the kinetic energy per nucleon in symmetric nuclear matter

$$E_{kin}(\rho, 0) = \frac{3\hbar^2}{10m} \left(\frac{3\pi^2\rho}{2} \right)^{2/3} \quad (3)$$

and $V_2(\rho)$ is the deviation of the interaction energy of pure neutron matter from that of symmetric nuclear matter. The $E_{sym}(\rho)$ becomes negative if the condition [35]

$$V_2(\rho) \leq -\frac{5}{9}E_{kin}(\rho, 0) \quad (4)$$

is reached at high densities. A negative symmetry energy at high densities implies that the pure neutron matter becomes the most stable state leading to the onset of the isospin separation instability (ISI). Consequently, pure neutron domains or neutron bubbles surrounding isolated protons may be formed in the cores of neutron stars [35]. Energetic nuclear reactions with rare isotopes provide a unique opportunity to pin down the $E_{sym}(\rho)$ at high densities and study the possible existence of ISI and its consequences. We use the following two representatives of the symmetry energy as predicted by many body theories

$$E_{sym}^a(\rho) \equiv E_{sym}(\rho_0)u \quad (5)$$

and

$$E_{sym}^b(\rho) \equiv E_{sym}(\rho_0)u \cdot \frac{u_c - u}{u_c - 1}, \quad (6)$$

where $u \equiv \rho/\rho_0$ and $u_c = \rho_c/\rho_0$ is the reduced critical density at which the $E_{sym}^b(\rho)$ crosses zero and becomes negative at higher densities. The predicted value of u_c ranges from about 2.7 (Hartree-Fock with the Skyrme interaction Sp [34]) to 9 (variational many-body approach with the UV14+UVII interaction [17]). For our numerical calculations in the following we use $u_c = 3$. Our conclusions in this work are qualitatively independent of this value. Thus future comparisons with experiments may rule out the existence of ISI below this density, but they can not exclude the occurrence of ISI at higher densities. By using higher values for u_c , effects found here will be simply shifted to higher beam energies. Therefore, excitation function studies in both theories and experiments will be necessary to determine the exact value of u_c if it does exist in nature. The above two forms of $E_{sym}(\rho)$ are shown in the upper window of Fig. 1. By design, they both have the same value of $E_{sym}(\rho_0) = 30$ MeV at the normal nuclear matter density ρ_0 and are very close to each other at lower densities. At high densities they have completely different trends reflecting the diverging predictions of nuclear many-body theories.

It is necessary to mention that in a recent publication [47], it was found that the symmetry energy itself is isospin-dependent at all densities. This amounts to absorbing the higher order

terms in δ into the E_{sym} in the expansion of the EOS of neutron-rich matter in Eq.(1). Because of the charge symmetry of nuclear interactions used the odd terms in δ should vanish. The lowest order correction to the parabolic approximation in Eq. (1) is the δ^4 term. The magnitude of the latter has been found extremely small in all microscopic many-body calculations (see, in particular those in refs. [11,12,17,18,48,49]), except that in [47]. The origin of the unusual prediction in the latter deserves further investigations. In this work we stick to the parabolic approximation of the EOS of neutron-rich matter.

B. Symmetry energy and proton fraction in neutron stars at β equilibrium

The above two forms of the symmetry energy lead to significantly different predictions on several properties of neutron stars. To a good approximation suitable for this study, a neutron star without neutrino trappings can be considered as a *npe*-matter consisting of neutrons (n), protons (p) and electrons (e). Through the direct ($n \rightarrow p + e + \bar{\nu}_e$) and/or standard ($n + n \rightarrow n + p + e + \bar{\nu}_e$) URCA processes the β equilibrium

$$n \leftrightarrow p + e^- + \bar{\nu} \quad (7)$$

can be established. The equilibrium condition requires that the respective chemical potentials to satisfy

$$\mu_n = \mu_p + \mu_e + \mu_{\bar{\nu}}, \quad (8)$$

and the charge neutrality requires that

$$\rho_p = \rho_e. \quad (9)$$

Since neutrinos do not accumulate in neutron stars a few seconds after their birth $\mu_{\bar{\nu}} = 0$. Within the Fermi gas model one then finds from Eqs. 8 and 9 the proton fraction $x_\beta \equiv \rho_p/(\rho_n + \rho_p)$ in neutron stars is determined by [39]

$$\hbar c(3\pi^2\rho x_\beta)^{1/3} = 4E_{sym}(\rho)(1 - 2x_\beta). \quad (10)$$

The equilibrium proton fraction is therefore entirely determined by the $E_{sym}(\rho)$. The values of x_β corresponding to the two chosen forms of symmetry energy are shown in the lower window of Fig. 1. With the $E_{sym}^b(\rho)$, the x_β is zero for $\rho/\rho_0 \geq 3$, indicating that a pure neutron matter could become most stable, leading to the isospin separation instability in HD neutron-rich matter. The value of x_β influences many other properties of neutrons stars, such as the cooling rate of protoneutron stars [39]. The fast cooling mechanism through the direct URCA process can happen if x_β is larger than about 1/9. It is seen that with the $E_{sym}^a(\rho)$, the neutron star becomes so proton-rich that the fast cooling can happen at densities higher than about $2.3\rho_0$. On the contrary, it is impossible for this process to happen with the $E_{sym}^b(\rho)$.

C. Equation of state of neutron-rich matter

With the two forms of the symmetry energy $E_{sym}^a(\rho)$ and $E_{sym}^b(\rho)$, the corresponding EOS for neutron-rich matter is rather different. To illustrate this point, the simplest, momentum-independent parameterization

$$e(\rho, 0) = \frac{a}{2}u + \frac{b}{1+\sigma}u^\sigma + \frac{3}{5}e_F^0 u^{2/3} \quad (11)$$

is used as the isoscalar part of the EOS, where $u \equiv \rho/\rho_0$ is the reduced density and $e_F^0 = 36$ MeV is the Fermi energy. The parameters $a = -358.1$ MeV, $b = 304.8$ MeV and $\sigma = 7/6$ are determined by saturation properties and a compressibility $K_\infty = 201$ MeV of isospin symmetric nuclear matter. Our conclusions in this work are qualitatively independent of the particular form of $e(\rho, 0)$. The use of a stiffer EOS, such as $K_\infty = 380$ MeV, will reduce the compression by about 15% in the energy range studied in this work. This will then simply shift the observed isospin effects to slightly higher beam energies. Shown in Fig. 2 are the EOS of isospin asymmetric nuclear matter with the $E_{sym}^a(\rho)$ (upper window) and $E_{sym}^b(\rho)$ (lower window), respectively. With the linearly increasing $E_{sym}^a(\rho)$, the EOS becomes stiffer with the increasing δ . The isospin symmetric nuclear matter remains to be

the ground state at all densities. This is in stark contrast to the situation using the $E_{sym}^b(\rho)$. The EOS obtained with the latter is softened instead of being stiffened by the increasing isospin asymmetry δ at densities higher than $3\rho_0$. At these high densities, in agreement with the information extracted from Fig. 1, the pure neutron matter becomes the most stable state whereas the isospin symmetric nuclear matter becomes the most unstable state of HD nuclear matter.

D. Nuclear symmetry potentials and their softest lines

In accordance with the EOS discussed above, the isoscalar potential is

$$v_0(\rho) = au + bu^\sigma \quad (12)$$

and the symmetry potentials can be obtained from

$$v_{asy}^q = \frac{\partial W_{asy}}{\partial \rho_q} \quad (13)$$

where q =neutrons and q =protons, respectively. The symmetry potential energy density W_{asy} is

$$W_{asy} = V_2 \rho \delta^2 = [E_{sym}(\rho) - c_1 u^{2/3}] \rho \delta^2, \quad (14)$$

where $c_1 = 3/5 e_F^0 (2^{2/3} - 1) \approx 12.7$ MeV. With the $E_{sym}^a(\rho)$ one obtains

$$v_{asy}^a = \pm 2(E_{sym}(\rho_0) - c_1)u\delta, \quad (15)$$

where “+” and “-” signs are for neutrons and protons, respectively. With the $E_{sym}^b(\rho)$, the symmetry potential is

$$v_{asy}^b = \pm 2(c_2 u_c u - c_2 u^2 - c_1 u^{2/3})\delta + (1/3 c_1 u^{2/3} - c_2 u^2)\delta^2, \quad (16)$$

where $c_2 = E_{sym}(\rho_0)/(u_c - 1) \approx 15$ MeV. At low densities v_{asy}^a and v_{asy}^b are very close since

$$\begin{aligned} \lim_{u \leq 1} v_{asy}^b &\approx \pm 2 [c_2(u_c - u) - c_1 u^{-1/3}] u \delta \\ &\approx \pm 2 [c_2(u_c - 1) - c_1] u \delta \\ &= \pm 2(E_{sym}(\rho_0) - c_1)u\delta = v_{asy}^a. \end{aligned} \quad (17)$$

This is so because of our choice of the two forms of the symmetry energy with the desire to study its HD behaviour. This feature is further illustrated in Fig. 3 where the above two symmetry potentials are shown as a function of density for $\delta = 0.2$ and $u_c = 3$. As one expects the symmetry potentials are rather similar at $\rho \leq \rho_0$ but very different at higher densities for both neutrons and protons. The different HD behaviour is expected to cause neutrons and protons to behave differently during the dynamical evolution of heavy-ion collisions.

Our main purpose in the following will be searching for signs of the different symmetry potentials in experimental observables of high energy heavy-ion collisions by comparing results for neutrons and protons and using different symmetry potentials. Of course, what is more important for the reaction dynamics is the force, or the slope of potentials. With the $E_{sym}^a(\rho)$ the repulsive (attractive) symmetry potential for neutrons (protons) increases linearly. With the $E_{sym}^b(\rho)$, however, the symmetry potential for neutrons (protons) has a broad maximum (minimum) around $\rho = 1.2\rho_0$ ($\rho = 1.4\rho_0$). Thus for both neutrons and protons the forces due to the symmetry potentials are zero around the extreme of their respective symmetry potentials. This property then leads to a *softest point* in the resultant EOS at a given δ for isospin asymmetric nuclear matter. Generally, for a varying δ there is a *softest line* for both neutrons and protons. These lines are determined by the condition

$$(\partial v_{asy}^b / \partial \rho)_\delta = 0. \quad (18)$$

With the $E_{sym}^b(\rho)$ these lines are along

$$\delta_{softest} = \pm \frac{6c_1 + 18c_2 u^{4/3} - 9c_2 u_c u^{1/3}}{c_1 - 9c_2 u^{4/3}}, \quad (19)$$

where the \pm sign is for neutrons/protons. These *softest lines* in neutron-rich matter are shown in Fig. 4. In heavy-ion collisions with a proper combination of the beam energy and isospin asymmetry, the system can cross these softest lines. The crossing points may manifest themselves as local minima in the excitation functions of collective flow for both neutrons and protons. This expectation is analogous to that for the local minimum in the

excitation function of transverse flow due to the Quark-Gluon-Plasma induced softening of the EOS in ultra-relativistic heavy-ion collisions [50]. The Coulomb potential may shift the relative values and slopes of proton potentials depending on the dynamical evolution of the charge distributions during the reaction. It is just difficult to predict quantitatively where the minima may appear based on the discussions of the symmetry potentials. Fortunately, transport models provide a reliable tool to make more quantitative predictions possible.

III. ISOSPIN ASYMMETRY OF DENSE NUCLEAR MATTER FORMED IN HIGH ENERGY HEAVY-ION COLLISIONS

High energy heavy-ion collisions provide the only terrestrial situation where the HD neutron-rich matter can be formed. Moreover, fast radioactive heavy-ion beams to be available at the planned Rare Isotope Accelerator (RIA) in the United States can make the HD nuclear matter even more neutron-rich [51]. The HD behaviour of $E_{sym}(\rho)$ affects properties of the HD nuclear matter formed in high energy heavy-ion collisions. Moreover, interesting precursors of the ISI might be observed in collisions with energetic neutron-rich nuclei.

A. Summary of an isospin-dependent hadronic transport model

We investigate the effects and phenomena mentioned above within an isospin-dependent hadronic transport model for an interacting system of nucleons, Delta resonances and pions [31,52,53]. Evolutions of the phase-space distribution functions of nucleons, Delta resonances and pions with their explicit isospin degrees of freedom are solved numerically by using of the test-particle approach [54,55]. Isospin-dependent total and differential cross sections among all particles are taken either from the elementary particle scattering data or obtained by using the detailed balance [56,57]. Explicitly isospin-dependent Pauli blockings for fermions are also employed. For a review of the model, we refer the reader to refs. [4,58].

At beam energies above the pion production threshold, baryon resonances play an important role in the reaction dynamics. In this study we limit ourselves to beam energies less than 2

GeV/nucleon. It is worth mentioning that for medium sized rare isotopes, such as ^{32}Na , high energy beams up to about 950 MeV/nucleon are currently available at GSI and for heavy rare isotopes, such as ^{132}Sn , beams up to 400 MeV/nucleon will be available at the future RIA. In this energy range, the most important baryon resonance is the $\Delta(1232)$. Shown in Fig. 5 are two examples of the multiplicities of $\Delta(1232)$ resonances and pions. The maximum population of the $\Delta(1232)$ is about 2% and 20% in the $^{132}\text{Sn} + ^{124}\text{Sn}$ reaction at an impact parameter of 1 fm and a beam energy of 400 and 2000 MeV/nucleon, respectively. The mean field potentials of pions and baryon resonances in nuclear matter are still largely unknown. We thus make here a minimum assumption that the isoscalar part of the Δ potential is the same as that for nucleons. To be consistent with the modeling of the isovector potential for nucleons, we assume that the isovector potential for Δ resonances is an average of that for neutrons and protons. The weighting factor depending on the charge state of the resonance is the square of the Clebsch-Gordon coefficients for isospin coupling in the processes $\Delta \leftrightarrow \pi N$. Thus, we have

$$v_{asy}(\Delta^-) = v_{asy}(n), \quad (20)$$

$$v_{asy}(\Delta^0) = \frac{2}{3}v_{asy}(n) + \frac{1}{3}v_{asy}(p), \quad (21)$$

$$v_{asy}(\Delta^+) = \frac{1}{3}v_{asy}(n) + \frac{2}{3}v_{asy}(p), \quad (22)$$

$$v_{asy}(\Delta^{++}) = v_{asy}(p). \quad (23)$$

Similarly, we define the effective isospin asymmetry δ_{like} for excited baryonic matter as

$$\delta_{like} \equiv \frac{(\rho_n)_{like} - (\rho_p)_{like}}{(\rho_n)_{like} + (\rho_p)_{like}}, \quad (24)$$

where

$$(\rho_n)_{like} = \rho_n + \frac{2}{3}\rho_{\Delta^0} + \frac{1}{3}\rho_{\Delta^+} + \rho_{\Delta^-}, \quad (25)$$

$$(\rho_p)_{like} = \rho_p + \frac{2}{3}\rho_{\Delta^+} + \frac{1}{3}\rho_{\Delta^0} + \rho_{\Delta^{++}}. \quad (26)$$

It is evident that the δ_{like} reduces naturally to δ as the beam energy becomes smaller than the pion production threshold.

B. Isospin asymmetry of dense matter formed in high energy heavy-ion collisions

Shown in Fig. 6 is the evolution of the central baryon density for the reaction of $^{132}\text{Sn} + ^{124}\text{Sn}$ at an impact parameter of 1 fm and beam energies of 200, 400, 1000 and 2000 MeV/nucleon, respectively. In this energy range a compression of about 1.7 to 3.7 times the normal nuclear matter density is reached. This very reaction at beam energies upto about 400 MeV/nucleon will be available at the RIA facility [51]. One notices that the $E_{sym}^b(\rho)$ leads to a slightly higher compression of about 10-15%. This is due to the relatively softened nuclear EOS with the E_{sym}^b than that with the E_{sym}^a .

Is the compressed hadronic matter neutron-rich or -poor compared to the initial reaction system? The answer to this question has important implications to several critical questions in nuclear astrophysics. To answer this question we show in Fig. 7 the correlation between the baryon density and the isospin asymmetry δ_{like} over the entire reaction volume at the time of about the maximum compression in the central $^{132}\text{Sn} + ^{124}\text{Sn}$ reactions with E/A=400 (middle window) and 2000 (bottom window) MeV/nucleon, respectively. The whole reaction volume is divided into cubic cells of 1 fm³ in size. Each point in the scatter plot represents one such cell. For a comparison, the correlation in the initial state of the reaction is shown in the upper window. The initial state for our transport model calculations is generated by using neutron and proton density profiles predicted by the Relativistic Mean Field model [14,59]. The average δ of the initial reaction system is 0.22, the low density tail extending to the far more neutron-richer side is due to the neutron skin in both the target and projectile nuclei. Thus a significant number of cells with densities close to $\rho/\rho_0 = 1$ have isospin asymmetries less than 0.22. How this initial $\rho - \delta$ correlation evolves in a heavy-ion collision depends sensitively on the HD behaviour of nuclear symmetry energy. With the $E_{sym}^a(\rho)$ the trend of continuous neutron distillation from higher density regions to lower ones persists at all energies. The high density region around $\rho = 2\rho_0$ is about twice more isospin symmetric than that with the $E_{sym}^b(\rho)$ at 400 MeV/nucleon. Most interestingly, with the $E_{sym}^b(\rho)$ the onset of ISI is clearly seen as indicated by the right turn of δ_{like} to higher values at $\rho \geq 3\rho_0$

in the reaction at $E_{beam}/A = 2$ GeV/nucleon.

The reason behind the observed neutron-distillation from the HD baryonic matter can be easily understood from the density dependence of symmetry energy shown in the upper window of Fig. 1. For two parts (1 and 2) of isospin asymmetric nuclear matter to be in chemical equilibrium the condition

$$E_{sym}(\rho_1)\delta_1 = E_{sym}(\rho_2)\delta_2 \quad (27)$$

must be satisfied [60–63]. Thus, it is energetically favorable in a dynamical process to have a migration of nucleons with its direction determined by Eq. 27 according to the density dependence of the $E_{sym}(\rho)$. With the $E_{sym}^a(\rho)$ which increases linearly with ρ , there is a continuous migration of neutrons (protons) from higher (lower) to lower (higher) densities. Whereas with the $E_{sym}^b(\rho)$ which peaks at $u = 1/2u_c$, it is most energetically favorable to deplete (concentrate) all neutrons (protons) from (to) the peak. Moreover, at $u \geq u_c$ the ISI sets in. It leads to an unlimited trapping of neutrons above the critical density $u_c = 3$.

To be more clear about the roles of the density dependent symmetry energy we investigate in Fig. 8 the average (over all cells of the same density) δ_{like} as a function of density for the central $^{132}Sn + ^{124}Sn$ reactions at 400 and 2000 MeV/nucleon. The overall rise of δ at low densities is mainly due to the neutron skins of the colliding nuclei and the distilled neutrons. Effects due to the different symmetry energies are more clearly revealed especially at high densities. For a comparison and study implications of our results to nuclear astrophysics, the $\rho - \delta$ correlation in neutron stars at β equilibrium is shown in the insert of Fig. 8. The isospin asymmetry at β equilibrium $\delta_\beta = 1 - 2x_\beta$ is completely determined by the $E_{sym}(\rho)$. With the $E_{sym}^b(\rho)$, the δ_β is 1 for $\rho/\rho_0 \geq 3$, indicating that the neutron star has become a pure neutron matter at these high densities. On the contrary, with the $E_{sym}^a(\rho)$, the neutron star becomes more proton-rich as the density increases. An astonishing similarity is seen in the resultant $\delta - \rho$ correlations for the neutron star and the heavy-ion collision. In both cases, the symmetry energy $E_{sym}^b(\rho)$ makes the HD nuclear matter more neutron-rich than the $E_{sym}^a(\rho)$ and the effect grows with the increasing density. Of course,

this is no surprise since the same underlying nuclear EOS is at work in both cases. The decreasing $E_{sym}^b(\rho)$ above $\frac{1}{2}u_c = 1.5\rho_0$ makes it more energetically favorable to have the denser region more neutron-rich.

The above analyses of the main features are at the instants of about the maximum compressions. How do they evolve in time? To answer this question the average n/p ratio of the HD region with $\rho/\rho_0 \geq 1$ is shown as a function of time and beam energy in Fig. 9. The effect on $(n/p)_{\rho/\rho_0 \geq 1}$ due to the different $E_{sym}(\rho)$ is seen to grow with the reaction time until the expansion has lead the system to densities below ρ_0 , especially at higher beam energies. Although the compression starts at about the same time, the expansion starts on a faster time scale at higher beam energies as one expects. Again, it is seen that whether the HD region is neutron-rich or -poor depends critically on the HD behaviour of nuclear symmetry energy.

C. Pion production effects on n/p ratio of dense matter

During heavy-ion collisions there is a net conversion of neutrons to protons due to the more abundant production of π^- 's than π^+ 's. It is therefore also interesting to explore effects of pion production on the n/p ratio of dense matter. This study is also necessary to be certain about the effects of the HD nuclear symmetry energy. We thus compare in Fig. 10 the HD n/p ratio with and without including the pion production channel in the central $^{132}\text{Sn} + ^{124}\text{Sn}$ reaction at a beam energy of 2 GeV/nucleon. The beam energy is chosen to illustrate the maximum effects of pion production since the latter decreases at lower beam energies. We artificially turned off the pion production channel, i.e., $N + N \rightarrow N + \Delta$, and attribute its cross section to elastic nucleon-nucleon scatterings such that the total reaction cross section is kept a constant. The central densities are shown in the upper rows of Fig. 10. It is seen that the overall compression is slightly reduced without including the pion production. This is because the latter has the role of enhancing the stopping power. It is interesting to note that the effect (difference between the curves a and b) on compression due

to the different symmetry energy is about the same with or without the pion production. The lower two rows demonstrate effects of pion production on the HD n/p ratio. By comparing the left and right windows of the lower two rows, it is seen that the pion production reduces the HD n/p ratios by about 15%, while the sensitivity to the symmetry energy remains almost the same. This finding also indicates that the pion production might be used as a perturbative probe of the n/p ratio of HD nuclear matter.

IV. PROBING THE HD BEHAVIOUR OF NUCLEAR SYMMETRY ENERGY WITH HIGH ENERGY HEAVY-ION COLLISIONS

How to probe experimentally the HD behaviour of $E_{sym}(\rho)$ in high energy heavy-ion collisions? In this section we study four complementary approaches. These are the π^-/π^+ ratio, nuclear transverse collective flow and its excitation function as well as the neutron-proton differential flow.

A. Pion probe

As we have shown in the previous section, that the pion production only affects perturbatively the n/p ratio of HD nuclear matter. On the other hand, at beam energies below about 2 GeV/nucleon, pions are mostly produced through the decay of $\Delta(1232)$ resonances. The primordial π^-/π^+ ratio is approximately quadratic in n/p according to the branching ratios of single pion production via Δ resonances in nucleon-nucleon collisions

$$\pi^-/\pi^+ = \frac{5n^2 + np}{5p^2 + np} \approx (n/p)^2. \quad (28)$$

Thus the π^-/π^+ ratio is expected to be a sensitive probe of the n/p ratio of HD nuclear matter. Pion reabsorptions and rescatterings ($\pi + N \rightarrow \Delta$ and $N + \Delta \rightarrow N + N$) are expected to complicate the above relationship. Nevertheless, very high sensitivity to the n/p ratio is retained in the final π^-/π^+ ratio as indicated in the experimental data of high energy heavy-ion collisions [64]. Shown in Fig. 11 are the $(\pi^-/\pi^+)_{like}$ ratio

$$(\pi^-/\pi^+)_{like} \equiv \frac{\pi^- + \Delta^- + \frac{1}{3}\Delta^0}{\pi^+ + \Delta^{++} + \frac{1}{3}\Delta^+} \quad (29)$$

as a function of time for the central $^{132}\text{Sn} + ^{124}\text{Sn}$ reaction at beam energies from 200 to 2000 MeV/nucleon. This ratio naturally becomes the final π^-/π^+ ratio at the freeze-out when the reaction time t is much longer than the lifetime of the delta resonance τ_Δ . The $(\pi^-/\pi^+)_{like}$ ratio is rather high in the early stage of the reaction because of the large numbers of neutron-neutron scatterings near the surfaces where the neutron skins of the colliding nuclei overlap. By comparing Fig. 9 and Fig. 11, it is seen that a variation of about 30% in the $(n/p)_{\rho/\rho_0 \geq 1}$ ratio due to the different $E_{sym}(\rho)$ results in about 15% change in the final π^-/π^+ ratio. It has thus an appreciable response factor of about 0.5 to the variation of HD n/p ratio and is approximately beam energy independent. Therefore, one can conclude that the $(\pi^-/\pi^+)_{like}$ ratio is a direct probe of the HD n/p ratio, and thus an indirect probe of the HD behaviour of nuclear symmetry energy.

B. Transverse collective flow and its excitation function

Next we investigate the transverse collective flow as a probe of the HD behaviour of nuclear symmetry energy. We perform the standard analysis of the average transverse momentum in the reaction plane [65]

$$\langle p_x/N \rangle (y) = \frac{1}{N(y)} \sum_{i=1}^{N(y)} p_{ix}(y), \quad (30)$$

where $N(y)$ is the number of particles at rapidity y and p_{ix} is i^{th} particle's transverse momentum in the reaction plane. Shown in Fig. 12 are two typical examples of the transverse collective flow analysis for neutrons and protons for the mid-central $^{132}\text{Sn} + ^{124}\text{Sn}$ reactions at 400 MeV/nucleon. Appreciable effects of the nuclear symmetry energy is clearly seen, especially for protons.

We found that the symmetry energy effects on the transverse flow vary with beam energy and are different for neutrons and protons. To better characterize the effects we study in

Fig. 13 the excitation function of flow parameter. The latter is defined as the slope of the transverse momentum distribution at mid-rapidity, i.e.

$$F \equiv \left(\frac{d \langle p_x / N \rangle}{dY_{cm} / y_{beam}} \right)_{y_{cm}=0}. \quad (31)$$

We concentrate on analyzing differences between the collective flows of neutrons and protons as well as those caused by using the different symmetry energies. These differences can be mainly attributed to the different symmetry potentials for neutrons and protons since the isoscalar potential has no direct contribution to these differences to the first order of approximation. On top of the generally growing flow parameter there are distinct structures closely associated with the symmetry energy used. In particular, a local minimum appears in the excitation functions for both neutrons and protons around $E_{beam}/A = 500$ MeV with the E_{sym}^b . The dip is more obvious for protons than neutrons. These minima are direct signals of the softening of the underlying EOS as we expected from studying the softest lines of the symmetry potentials. With the E_{sym}^a there is also a local minimum in the excitation function for protons around $E_{beam}/A = 300$ MeV. This minimum is a result of the interplay between repulsive hadronic scatterings and the attractive symmetry potential for protons (the solid line in the bottom window of Fig. 3). To be more quantitative, the average number of successful hadronic scatterings per nucleon and the maximum baryonic compression are shown as a function of beam energy in Fig. 14. Because the E_{sym}^b softens the EOS it thus leads to an about 3% higher compression and more scatterings compared to the case with the E_{sym}^a . The small increase in compression has very little effect on the scalar potential. Thus the observed structures can not be due to the isoscalar potentials. Below the pion production threshold in nucleon-nucleon collisions at about 296 MeV, the Pauli blocking is still strong and thus the collision numbers increase very little with beam energy. Whereas above the pion production threshold, because of the opening of the inelastic channel via $N + N \rightarrow N + \Delta$ and its resonance nature, the collision numbers grow quickly. With the E_{sym}^a , for protons the symmetry potential causes negative flow while the collisions result in positive flow. Around 300 MeV/nucleon the collision numbers are still small, effects of the

symmetry potential are thus relatively important in the interplay which leads to the dip near the pion production threshold. At higher beam energies, however, the flow increases because of the dominating role of the collisions and their fast growth with beam energy. While for neutrons with the E_{sym}^a , both the collisions and the repulsive symmetry potential (the solid line in the upper window of Fig. 3) enhance the transverse flow. Thus the flow parameter for neutrons increases almost monotonously with beam energy. Therefore, the structures observed above in the excitation functions of the nuclear transverse flow parameter are unique qualitative signatures of the density dependence of symmetry energy.

C. Neutron-proton differential flow probe

The neutron-proton differential collective flow is measured by [33]

$$F_{np}(y) \equiv \frac{1}{N(y)} \sum_{i=1}^{N(y)} p_{x_i} \tau_i, \quad (32)$$

where $N(y)$ is the total number of free nucleons at the rapidity y , p_{x_i} is the transverse momentum of particle i in the reaction plane, and τ_i is $+1$ and -1 for neutrons and protons, respectively. The free nucleons are identified as those having local nucleon densities less than $1/8\rho_0$. The $F_{np}(y)$ combines constructively the in-plane transverse momenta generated by the isovector potentials while reducing significantly influences of the isoscalar potentials of both neutrons and protons. Thus, it can reveal more directly the HD behaviour of $E_{sym}(\rho)$ in high energy heavy-ion collisions. Two typical results for mid-central $^{132}\text{Sn} + ^{124}\text{Sn}$ reactions at 400 MeV/nucleon and 1000 MeV/nucleon, respectively, are shown in Fig. 15. A clear signature of the HD behaviour of $E_{sym}(\rho)$ appears at both forward and backward rapidities. To characterize the effect, the slope $dF_{np}/d(y_{cm}/y_{beam})$ at mid-rapidity is shown as a function of beam energy in Fig. 16. A striking difference of about a factor of 2 exists in the reactions at $E_{beam} \geq 200$ MeV/nucleon. This large effect can be very easily observed by using available detectors at several heavy-ion facilities in the world. However, the interesting structures observed in the excitation function of the transverse flow parameter F is largely being

smearred out because the different rapidity distributions of neutrons and protons also enters in the calculation of the neutron-proton differential flow. Compared with the π^-/π^+ ratio, both the transverse flow and the neutron-proton differential collective flow are more directly affected by and are thus also more sensitive probes of the HD behaviour of $E_{sym}(\rho)$.

V. SUMMARY

In summary, the HD behaviour of nuclear symmetry energy has been puzzling physicists for decades. In this work, high energy heavy-ion collisions are proposed as a novel means to solve this longstanding problem. Within an isospin dependent hadronic transport model using two representative density dependent symmetry energy functions predicted by many body theories, it is shown that the isospin asymmetry of HD nuclear matter formed in high energy heavy-ion collisions is uniquely determined by the HD behaviour of $E_{sym}(\rho)$. It is demonstrated that the isospin separation instability indeed can happen in high energy heavy-ion collisions. We explored several promising experimental probes for the HD symmetry energy. Among them, four quantitatively sensitive observables, the π^-/π^+ ratio, nuclear transverse collective flow and its excitation function as well as the neutron-proton differential collective flow are studied. A precursor of the possible isospin separation instability in dense neutron-rich matter is predicted to appear as the local minima in the excitation functions of the flow parameter for both neutrons and protons above the pion production threshold. This precursor can be used as a unique signature of the isospin dependence of the nuclear EOS. This *qualitative* signature is advantageous over the other *quantitative* observables because the latter are often affected by several ingredients of the reaction dynamics and experimental uncertainties. It should be noted that the present study is based on a momentum-independent transport model. The momentum-dependent potential is known to be important for a reliable description of global momentum distributions. Nevertheless, we expect that all qualitative features, such as the existence of the minimum in the excitation function of transverse flow, are not affected by the momentum-dependence. However, the

quantitative results, such as the exact location of the flow minimum, are affected by the momentum-dependence of the nuclear potential. A more refined study using a momentum-dependent isoscalar potential is underway and the results will be reported elsewhere. It should also be mentioned that the fragmentation mechanism of isospin asymmetric nuclear matter is still not clear and remains a hot topic of current studies [66]. The different fragmentation mechanisms might affect the neutron/proton ratio of the observed free nucleons, and thus the neutron-proton differential flow. It would thus be useful to measure also observables associated with fragments together with the single particle observables examined in this study. It still remains a theoretical challenge to develop a fully quantum transport theory that deals with both particle production and cluster formation in a numerically tractable manner. The present work shows the need and promise of working in this direction. Experimental measurements of the proposed observables will provide the first terrestrial data to constrain stringently the HD behaviour of nuclear symmetry energy. Future comparisons between the experimental data and model calculations will allow us to extract crucial information about the EOS of dense neutron-rich matter.

This work was supported in part by the National Science Foundation Grant No. PHY-0088934 and Arkansas Science and Technology Authority Grant No. 00-B-14.

REFERENCES

- [1] A special volume of Nucl. Phys. **A693** (2001), Ed. I. Tanihata.
- [2] *Isospin Physics in Heavy-Ion Collisions at Intermediate Energies*, Eds. Bao-An Li and W. Udo Schröder, ISBN 1-56072-888-4, Nova Science Publishers, Inc (2001, New York).
- [3] R. Pak et al., Phys. Rev. Lett. **78**, 1026 (1997).
- [4] B.A. Li, C.M. Ko and W. Bauer, topical review, Int. Jou. Mod. Phys. **E7**, 147 (1998).
- [5] S.J. Yennello et al., Nucl. Phys. **A681**, 317c (2001).
- [6] M.B. Tsang, W.A. Friedman, C. Gelbke, W.G. Lynch, G. Verde and H. Xu, Nucl. Phys. **A681**, 323c (2001).
- [7] W. Udo Schröder and J. Töke, Nucl. Phys. **A681**, 418c (2001).
- [8] M. Di Toro, V. Baran, M. Colonna, S. Maccarone, M. Zielinska-Pfabe and H.H. Wolter, Nucl. Phys. **A681**, 426c (2001).
- [9] U. Lombardo and W. Zuo, Chapter 1 of the book in ref. [2].
- [10] K.A. Brueckner, S.A. Coon and J. Dabrowski, Phys. Rev. **168**, 1184 (1967).
- [11] P.J. Siemens, Nucl. Phys. **A141**, 225 (1970).
- [12] V.R. Pandharipande et al., Phys. Lett. **B38**, 608 (1972); B. Friedman et al., Nucl. Phys. **A361**, 502 (1981); I.E. Lagaris et al., Nucl. Phys. **A369**, 470 (1981).
- [13] S.A. Chin, Ann. Phys. (N.Y.), **108**, 301 (1977).
- [14] B.D. Serot and J.D. Walecka, Adv. Nucl. Phys. **16**, 1 (1986).
- [15] B. ter Haar and R. Malfliet, Phys. Rev. Lett. **59**, 1652 (1987).
- [16] H. Müther, M. Prakash and T.L. Ainsworth, Phys. Lett. **B199**, 469 (1987).
- [17] R.B. Wiringa, V. Fiks and A. Fabrocini, Phys. Rev. **C38**, 1010 (1988).

- [18] I. Bombaci and U. Lombardo, Phys. Rev. **C44**, 1892 (1991).
- [19] A. Akmal, V.R. Pandharipande and D.G. Ravenhall, Phys. Rev. **C58**, 1804 (1998).
- [20] H. Huber, F. Weber, and M.K. Weigel, Phys. Rev. **C57**, 3484 (1998).
- [21] W.D. Myers and W.J. Świątecki, Phys. Rev. **C57**, 3020 (1998).
- [22] C.-H. Lee, T.T.S. Kuo, G.Q. Li and G.E. Brown, Phys. Rev. **C57**, 3488 (1998).
- [23] K. Oyamatsu et al., Nucl. Phys. **A634**, 3 (1998).
- [24] B.A. Brown, Phys. Rev. Lett. **85**, 5296 (2000).
- [25] C.J. Horowitz and J. Piekarewicz, Phys. Rev. Lett. **86**, 5647 (2001); C.J. Horowitz et al., Phys. Rev. **C63**, 025501 (2001).
- [26] S. Typel and B.A. Brown, Phys. Rev. **C64**, 027302 (2001).
- [27] R.J. Furnstahl, preprint nucl-th/0112085.
- [28] B.A. Li, C.M. Ko and Z.Z. Ren, Phys. Rev. Lett. **78**, 1644 (1997).
- [29] H. Xu et al., Phys. Rev. Lett. **85**, 1908 (2000).
- [30] W.P. Tan et al, Phys. Rev. **C64**, R051901 (2001).
- [31] B.A. Li et al., Phys. Rev. Lett. **76**, 4492 (1996).
- [32] L. Scalone, M. Colonna and M. Di Toro, Phys. Lett. **B461**, 9 (1999).
- [33] B.A. Li, Phys. Rev. Lett. **85**, 4221 (2000).
- [34] J. Margueron, J. Navarro, N. Van Giai and W. Jing, nucl-th/0110026.
- [35] M. Kutschera, Phys. Lett. **B340**, 1 (1994); Z. Phys. **A348**, 263 (1994); Acta Phys. Polon. **B29**, 25 (1998).
- [36] J.M. Lattimer and M. Prakash, Astrophys J. **550**, 426 (2001).

- [37] M. Prakash et al., Phys. Rep. **280**, 1 (1997).
- [38] I. Bombaci, Chapter 2 of the book in ref. [2].
- [39] J.M. Lattimer et al., Phys. Rev. Lett. **66**, 2701 (1991).
- [40] K. Sumiyoshi and H. Toki, Astro. Phys. Journal, **422**, 700 (1994).
- [41] C.-H. Lee, Phys. Rep. **275**, 255 (1996) and references therein.
- [42] S. Kubis and M. Kutschera, Acta Phys. Polon. **B30**, 2747 (1999).
- [43] M. Prakash, T.L. Ainsworth and J.M. Lattimer, Phys. Rev. Lett. **61**, 2518 (1988).
- [44] L. Engvik et al., Phys. Rev. Lett. **73**, 2650 (1994).
- [45] M. Kutschera and J. Niemiec, Phys. Rev. **C62**, 025802 (2000).
- [46] B.A. Li, Phys. Rev. Lett. **88**, 192701 (2002).
- [47] F.L. Braghin, Nucl. Phys. **A696**, 413 (2001).
- [48] O. Sjöberg, Nucl. Phys. **A222**, 161 (1974).
- [49] G.H. Bordbar and M. Modarres, Phys. Rev. **C57**, 714 (1998).
- [50] C.M. Hung and E.V. Shuryak, Phys. Rev. Lett. **75**, 4003 (1995); D.H. Rischke et al., Heavy-Ion Phys. **1**, 309 (1995); B.A. Li and C.M. Ko, Phys. Rev. **C58**, 1382 (1998).
- [51] “Scientific Opportunities with Fast Fragmentation Beams from RIA”, NSCL/MSU report, March, 2000, <http://www.nscl.msu.edu/research/ria/whitepaper.pdf>.
- [52] B.A. Li and W. Bauer, Phys. Rev. **C44**, 450, (1991); B.A. Li, W. Bauer and G.F. Bertsch, *ibid*, **C44**, 2095 (1991).
- [53] B.A. Li, Phys. Lett. **B319**, 412 (1993).
- [54] C.Y. Wong, Phys. Rev. **C25**, 1461 (1982).

- [55] G.F. Bertsch and Subal Das Gupta, Phys. Rep. **160**, 189 (1988).
- [56] P. Danielewicz and G.F. Bertsch, Nucl. Phys. **A533**, 712 (1991).
- [57] B.A. Li, Nucl. Phys. **A552**, 605 (1993).
- [58] B.A. Li, A.T. Sustich, B. Zhang and C.M. Ko, Topical Review, Int. Jou. of Modern Phys. E10, 267 (2001).
- [59] Z.Z. Ren et al, Phys. ReV. **C52**, R20 (1995).
- [60] H. Müller and B.D. Serot, Phys. Rev. **C52**, 2072 (1995).
- [61] B.A. Li and C.M. Ko, Nucl. Phys. **A618**, 498 (1997).
- [62] V. Baran, A. Larionov, M. Colonna and M. Di Toro, Nucl. Phys. **A632**, 287 (1998).
- [63] L. Shi and P. Danielewicz, Euro. Phys. Lett. **49**, 34 (2000).
- [64] R. Stock, Phys. Rep. **135**, 259 (1986).
- [65] P. Danielewicz and G. Odyniec, Phys. Lett. **B157**, 146 (1985).
- [66] B.A. Li, A.T. Sustich, B. Zhang and M. Tilley, Nucl. Phys. **A699**, 493 (2002).

FIGURES

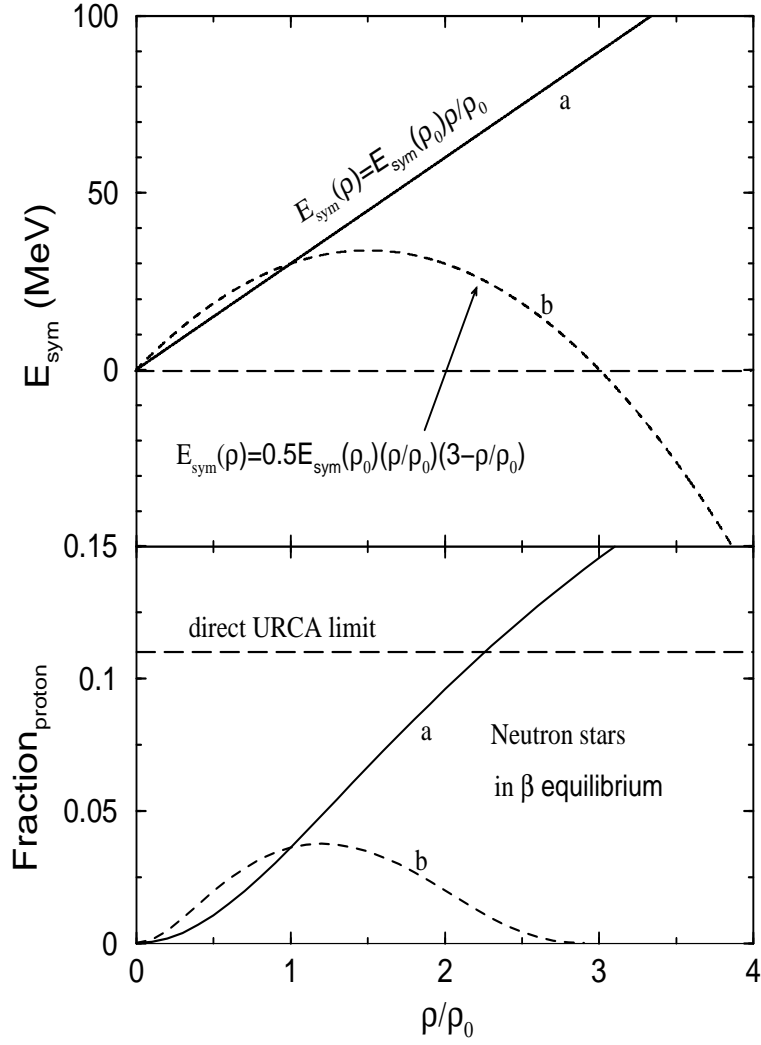


FIG. 1. Upper window: Two representatives of the nuclear symmetry energy as a function of density. Lower window: the corresponding proton fractions in neutron stars at β equilibrium.

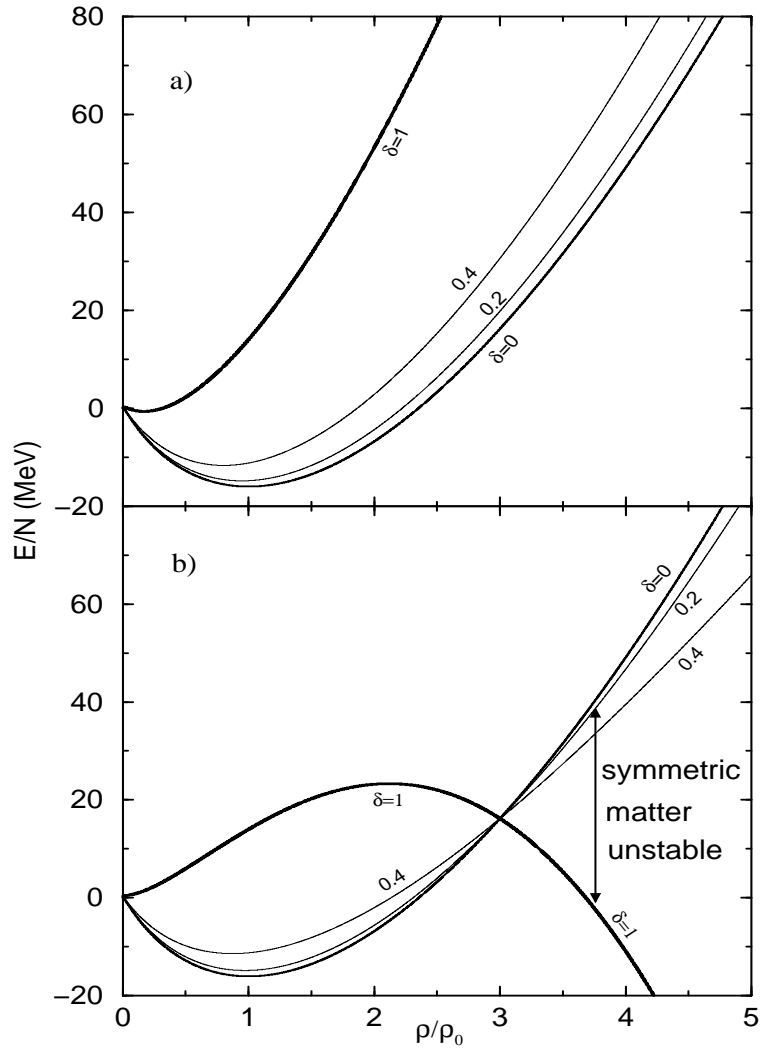


FIG. 2. The upper (lower) window is the equation of state of isospin-asymmetric nuclear matter using the nuclear symmetry energy parameterization E_{sym}^a (E_{sym}^b).

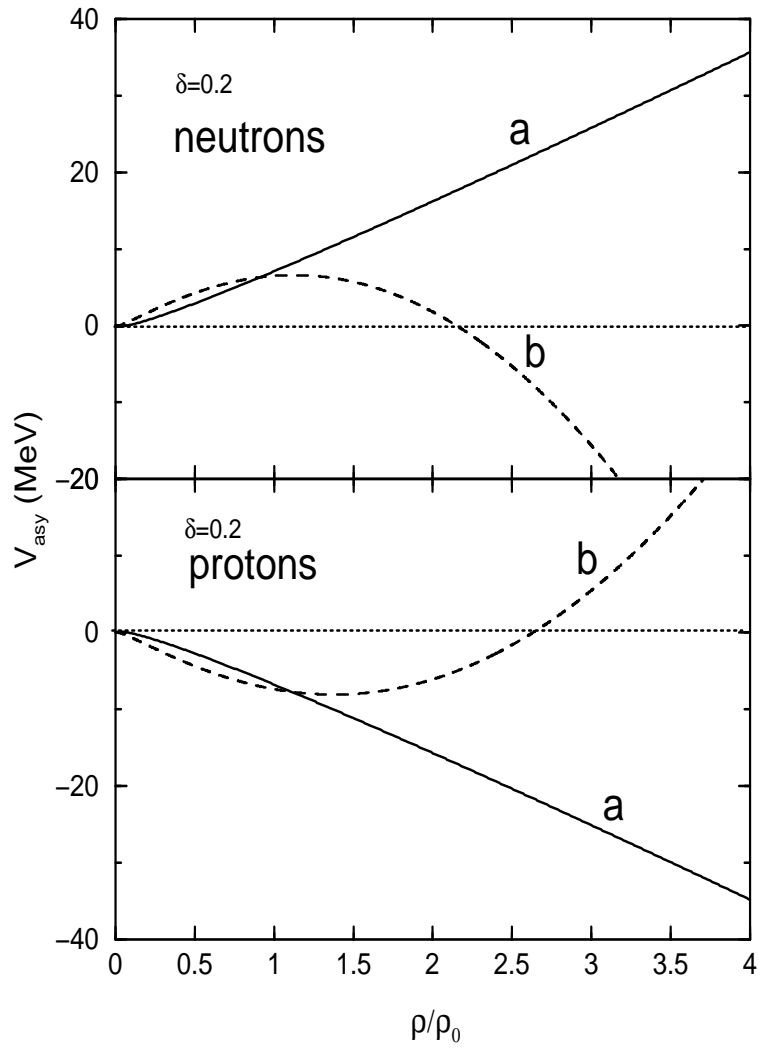


FIG. 3. Symmetry potentials for neutrons (upper window) and protons (lower window) using the nuclear symmetry energy E_{sym}^a and E_{sym}^b , respectively.

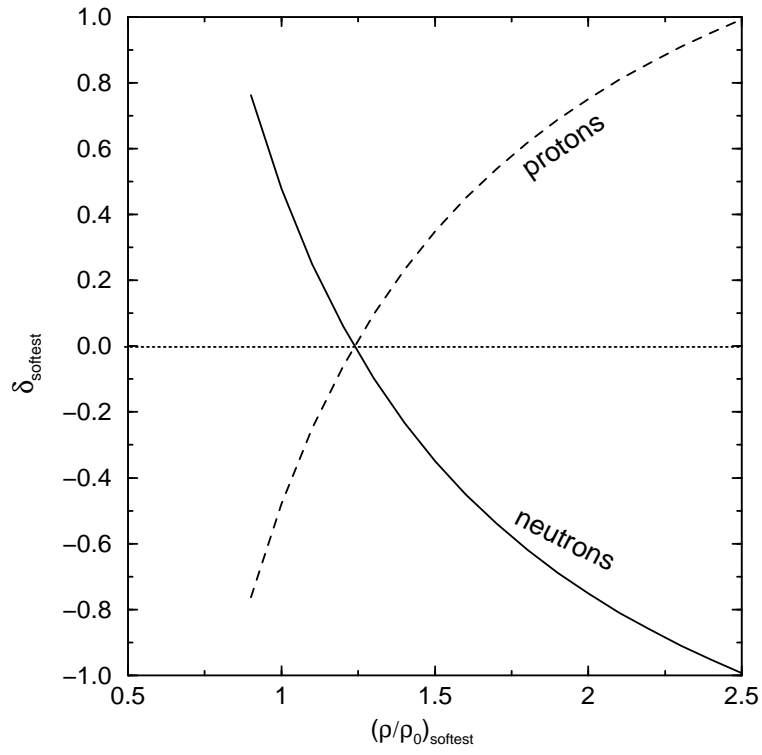


FIG. 4. The softest lines for neutrons and protons using the symmetry potential corresponding to the E_{sym}^b .

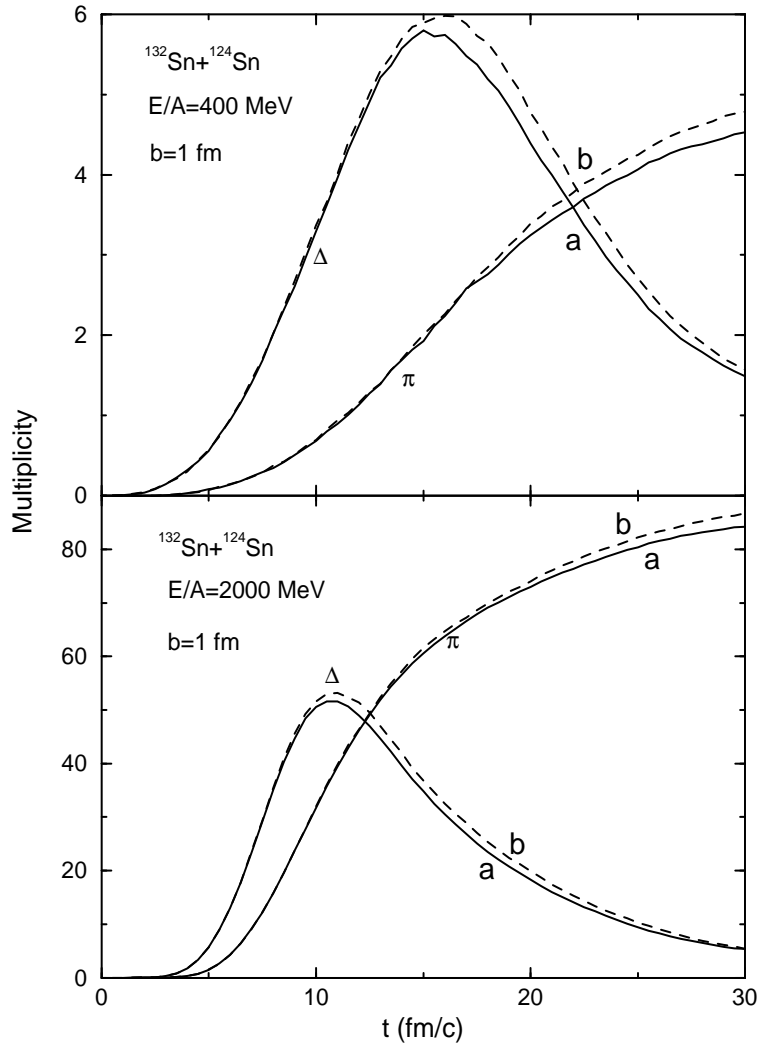


FIG. 5. Multiplicities of Delta resonances and pions in the central reaction of $^{132}\text{Sn} + ^{124}\text{Sn}$ at a beam energy of 400 MeV/nucleon (upper window) and 2 GeV/nucleon (lower window).

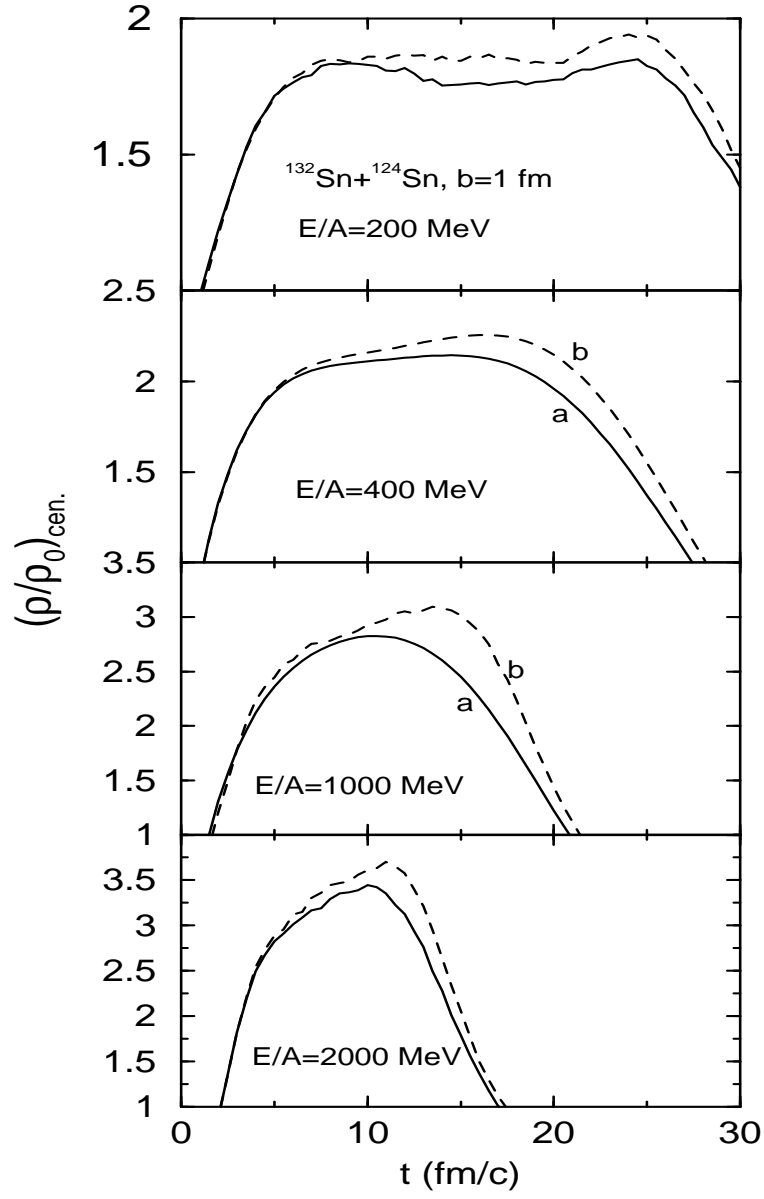


FIG. 6. Evolution of the central baryon density in the central reaction of $^{132}\text{Sn} + ^{124}\text{Sn}$ at a beam energy from 200 to 2000 MeV/nucleon.

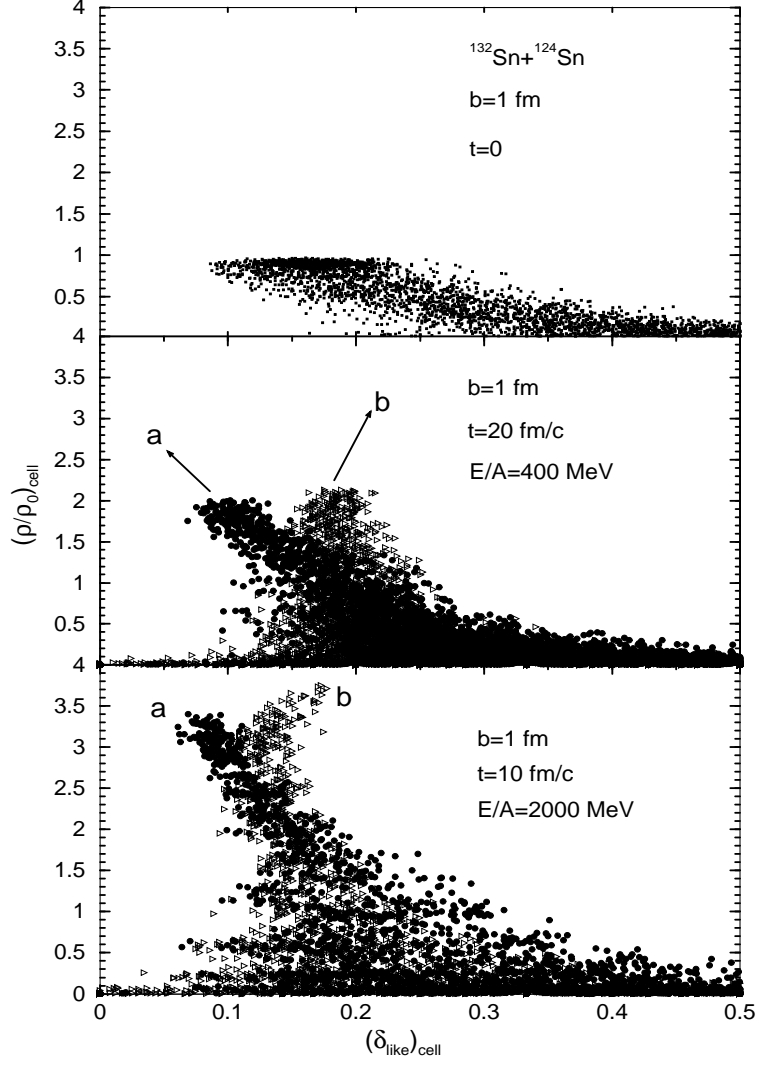


FIG. 7. Scatter plots of isospin asymmetry-density correlation in the initial state (upper window) and at the instants of maximum compressions in the reaction of $^{132}\text{Sn} + ^{124}\text{Sn}$ with the nuclear symmetry energy E_{sym}^a (filled circles) and E_{sym}^b (right triangles), respectively.

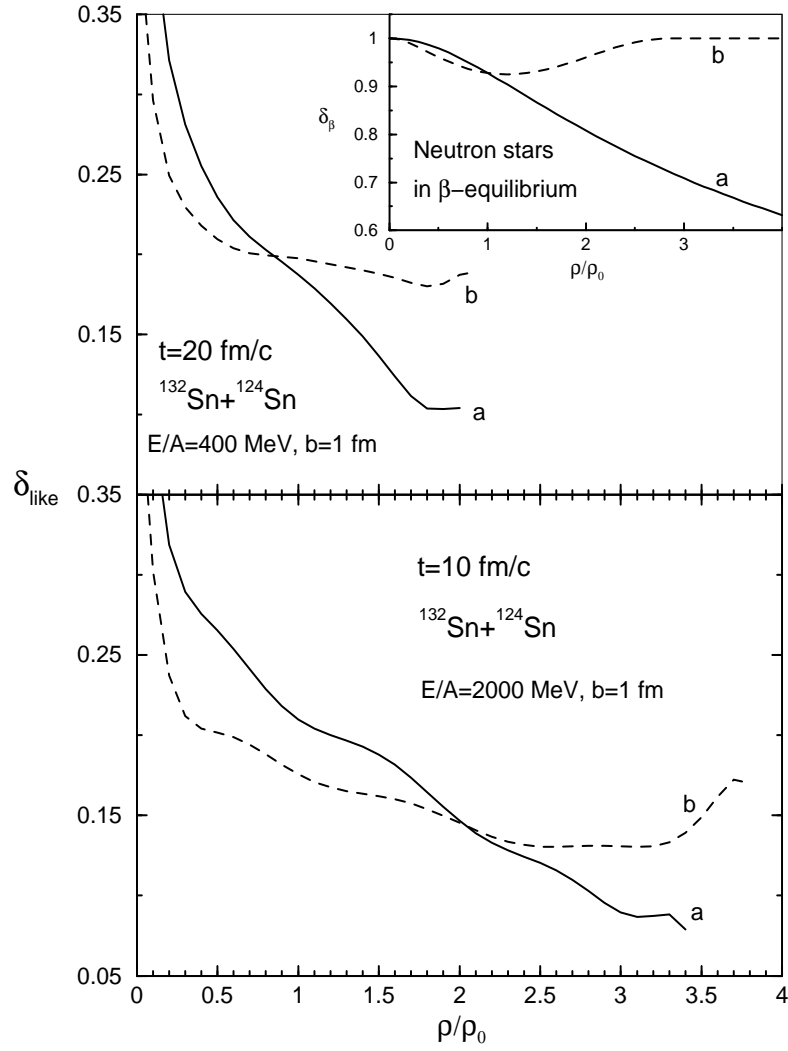


FIG. 8. Upper window: the isospin asymmetry-density correlations at $t=20$ fm/c and $E_{\text{beam}}/A = 400$ MeV in the central $^{132}\text{Sn} + ^{124}\text{Sn}$ reaction with the nuclear symmetry energy E_{sym}^a and E_{sym}^b , respectively. Lower window: the same correlation as in the upper window but at 10 fm/c and $E_{\text{beam}}/A = 2$ GeV/nucleon. The corresponding correlation in neutron stars is shown in the insert.

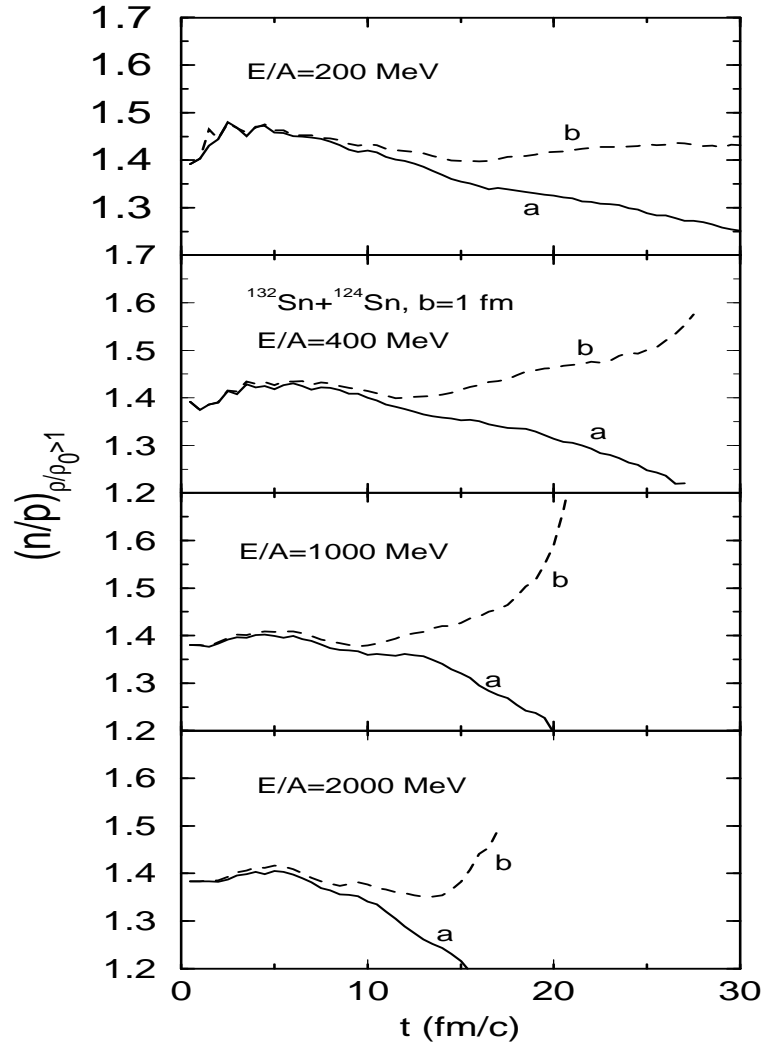


FIG. 9. The neutron/proton ratio of nuclear matter with density higher than the normal nuclear matter density as a function of time with the nuclear symmetry energy E_{sym}^a and E_{sym}^b , respectively.

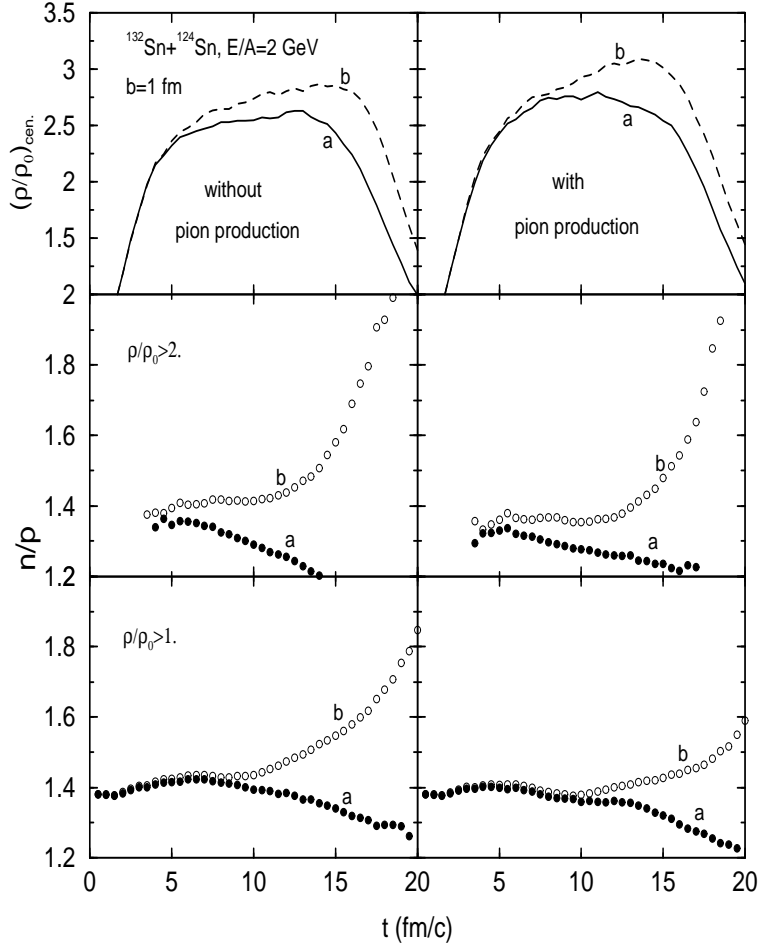


FIG. 10. Central baryon density (top row) and the neutron/proton ratio of nuclear matter with density $\rho \geq 2\rho_0$ (middle row) and $\rho \geq \rho_0$ (bottom row) with (right column) and without (left column) the pion production channel in the central $^{132}\text{Sn} + ^{124}\text{Sn}$ reaction at a beam energy of 2 GeV/nucleon.

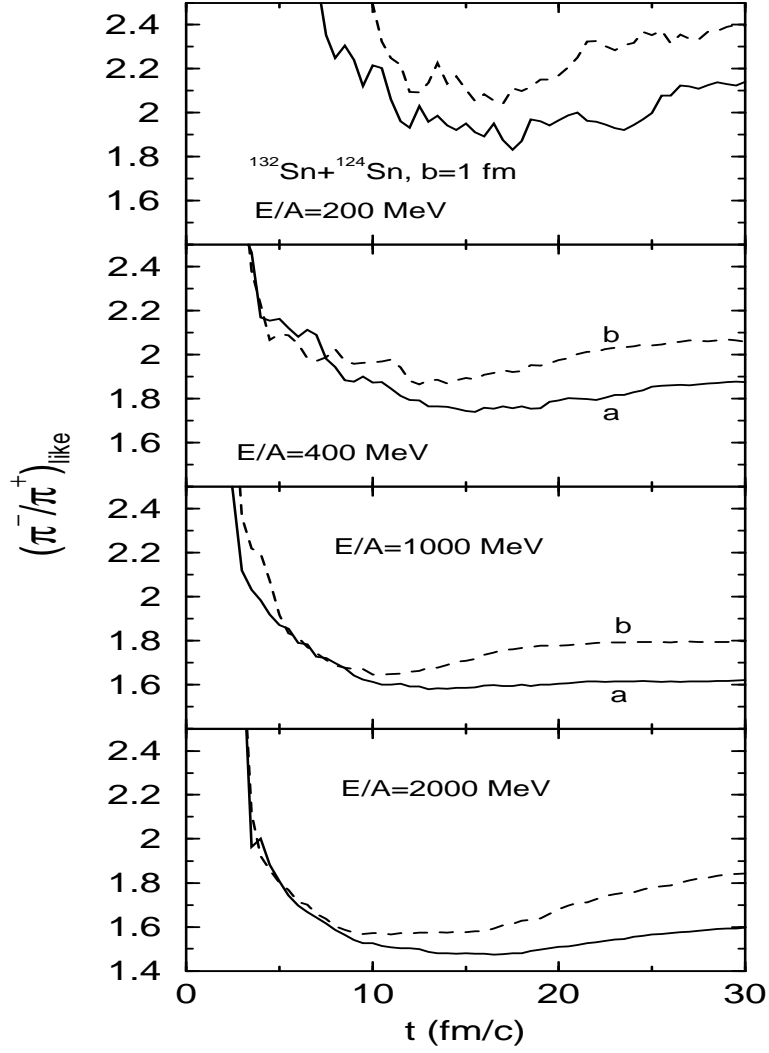


FIG. 11. π^-/π^+ ratio as a function of time in the central $^{132}\text{Sn} + ^{124}\text{Sn}$ reaction at a beam energy of between 200 and 2000 MeV/nucleon.

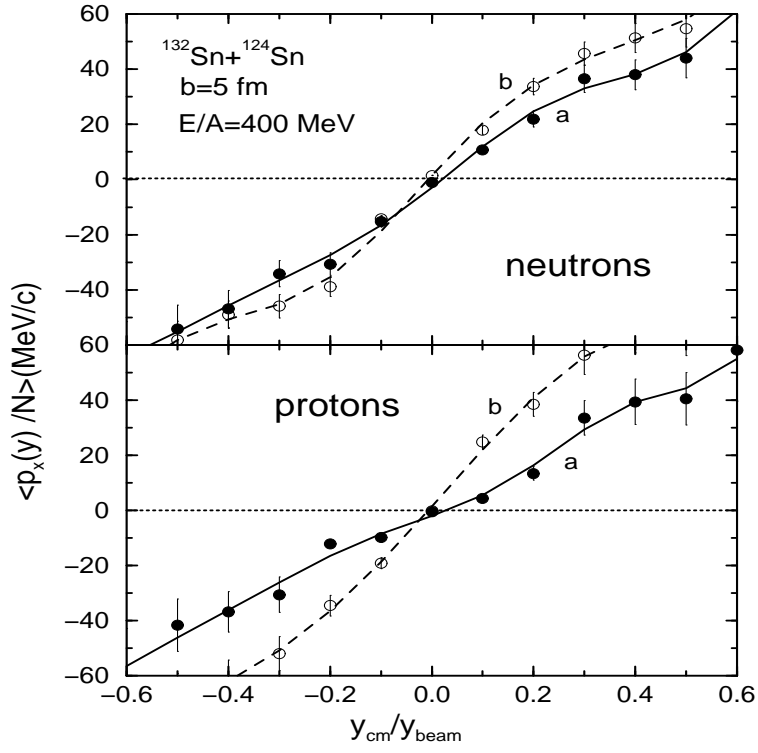


FIG. 12. Transverse flow analysis for neutrons (upper window) and protons (lower window) in the mid-central $^{132}\text{Sn} + ^{124}\text{Sn}$ reaction at a beam energy of 400 MeV/nucleon.

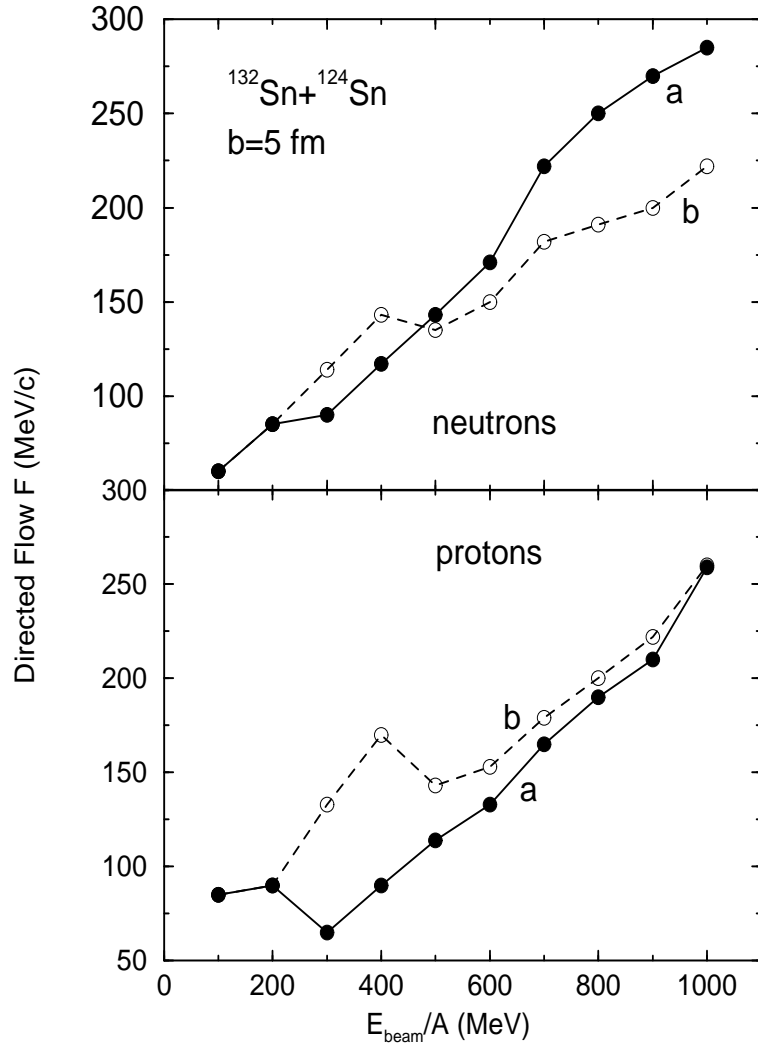


FIG. 13. The excitation functions of the transverse flow parameter for neutrons (upper) and protons (lower) in the mid-central $^{132}\text{Sn} + ^{124}\text{Sn}$ reactions.

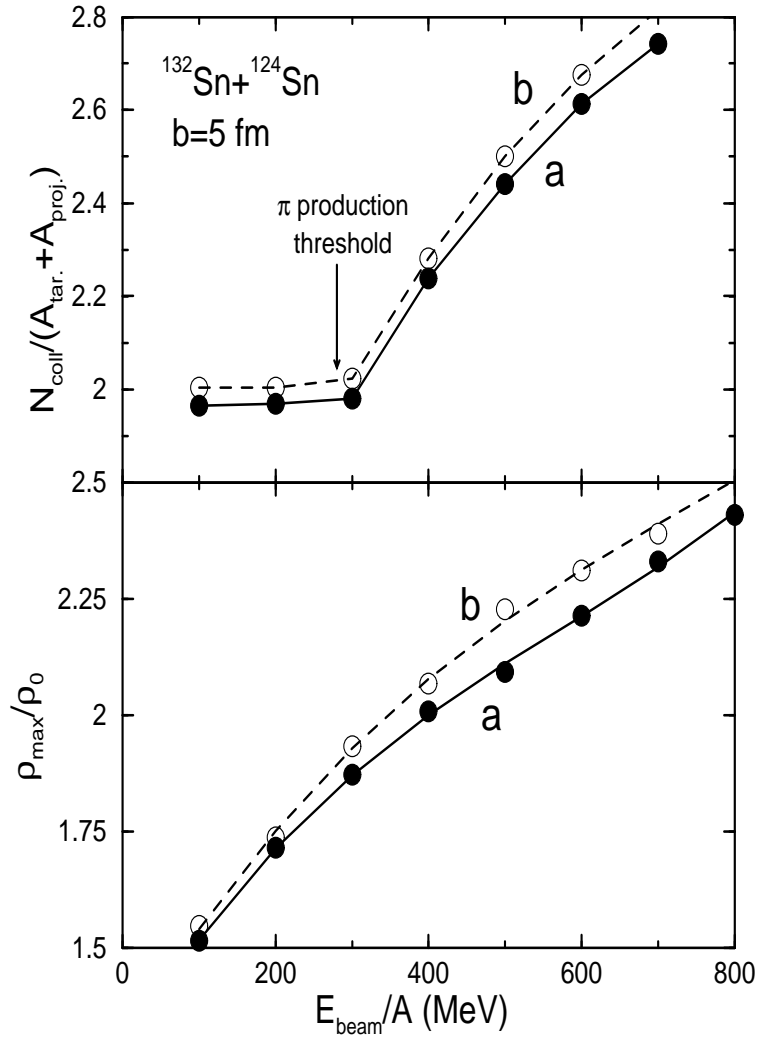


FIG. 14. The average number of successful hadronic scatterings per initial nucleon (upper) and the maximum baryon density reached in the mid-central $^{132}\text{Sn} + ^{124}\text{Sn}$ reaction as a function of beam energy.

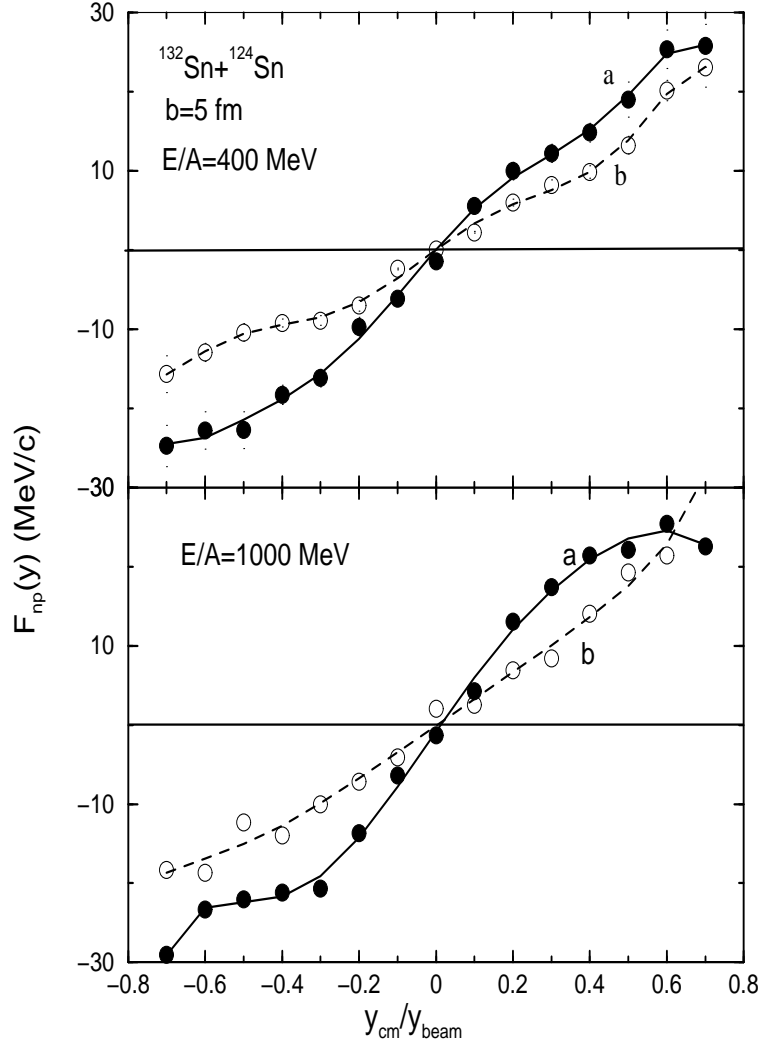


FIG. 15. The neutron-proton differential collective flow in the mid-central $^{132}\text{Sn} + ^{124}\text{Sn}$ reactions at $E_{beam}/A = 400$ MeV (upper window) and 1000 MeV (lower window) with the nuclear symmetry energy E_{sym}^a and E_{sym}^b , respectively.

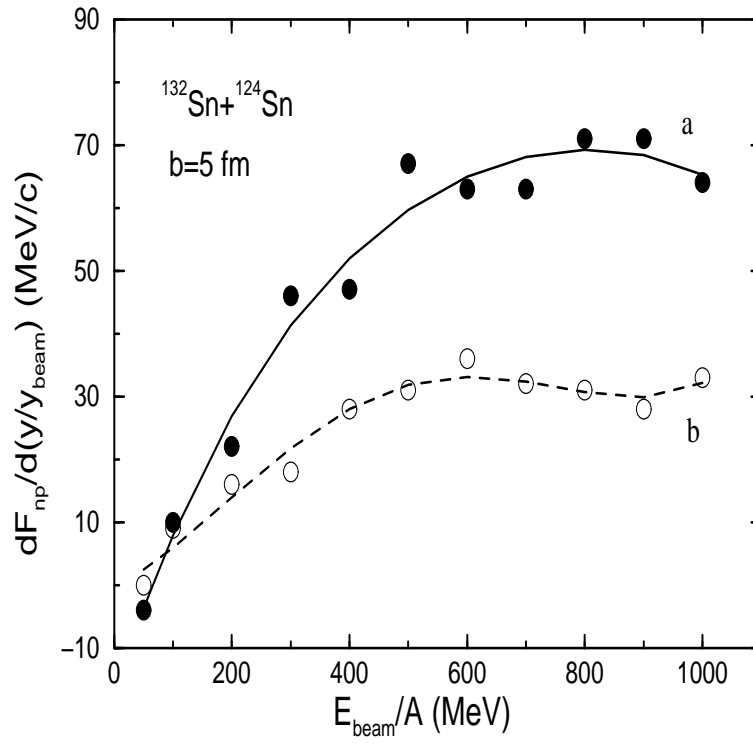


FIG. 16. Excitation function of the slope parameter of the neutron-proton differential flow for the mid-central $^{132}\text{Sn} + ^{124}\text{Sn}$ reaction. The lines are drawn to guide the eye